

**Measurement and comparison of distributional shift and its relation to rarity, poverty, and  
scarcity**

Kenneth J. Locey<sup>1\*</sup>, Brian D. Stein<sup>1</sup>

<sup>1</sup> Center for Quality, Safety and Value Analytics, Rush University Medical Center, Chicago,  
Illinois, 60612, USA.

\* Corresponding author. email: [Kenneth\\_J\\_Locey@rush.edu](mailto:Kenneth_J_Locey@rush.edu)

# **Measurement and comparison of distributional shift and its relation to rarity, poverty, and scarcity**

## **Abstract**

The comparison of frequency distributions is a common statistical task with broad applications. However, existing measures do not explicitly quantify the magnitude and direction by which one distribution is shifted relative to another. In the present study, we define distributional shift (DS) as the concentration of frequencies towards the lowest discrete class, e.g., the left-most bin of a histogram. We measure DS via the sum of cumulative frequencies and define relative distributional shift (RDS) as the difference in DS between distributions. Using simulated random sampling, we show that RDS is highly related to measures that are widely used to compare frequency distributions. Focusing on specific applications, we show that DS and RDS provide insights into healthcare billing distributions, ecological species-abundance distributions, and economic distributions of wealth. RDS has the unique advantage of being a signed (i.e., directional) measure based on a simple difference in an intuitive property that, in turn, serves as a measure of rarity, poverty, and scarcity.

Keywords: distance; frequency distribution; histogram; poverty; rarity; shift

## 1. Introduction

Comparisons of frequency distributions are common statistical tasks involving the measurement of differences between distributions, tests for goodness-of-fit against theoretical predictions and empirical benchmarks, as well as comparisons based on the calculation of descriptive measures (e.g., inequality, diversity) [1, 2, 5, 9-16, 23, 28]. Frequencies can be counts, percentages, or probability densities while their distributions may be continuous or discrete, cumulative or non-cumulative, and numerical or ordinal [9, 17]. Consequently, many statistical tests, indices, and other measures have been developed to enable the comparative analysis of frequency distributions (e.g., Table 1) [3, 4, 8, 9, 16, 28].

**Table 1.** Select measures used to compare frequency distributions. These measures are included in the current work.

Measure	Equation	Description
Chi-square Distance	$\frac{1}{2} \sum_{i=1}^k \frac{(f_{1i} - f_{2i})^2}{(f_{1i} + f_{2i})}$	One half the sum of squared differences between $k$ bins of two frequency distributions ( $f_1, f_2$ ) normalized by the sum of $f_{1i}$ and $f_{2i}$ [1].
Kolmogorov-Smirnov Distance	$\sup_x  F_1(x) - F_2(x) $	The maximum absolute difference between cumulative distribution functions [3].
Kullback-Leibler Divergence	$\sum_{i=1}^k f_{1i} \log \left( \frac{f_{1i}}{f_{2i}} \right)$	Also known as relative information entropy. Measures the expected logarithmic difference in frequencies for corresponding bins, as the average information gain per observation needed to distinguish between $f_1$ and $f_2$ . [3].
Histogram Intersection	$\sum_{i=1}^k \min(f_{1i}, f_{2i})$	Measures the sum of the minimum values at each bin, emphasizing shared values in distributions [3].
Earth Mover's Distance	$\min_{\gamma \in \Pi(P, Q)} \sum_{i,j} \gamma(i \cdot j) \cdot d(i, j)$	Measures dissimilarity between cumulative probability distributions by quantifying the minimum "work" required to transform one into another. The equation originates from optimal mass transportation [3].
Ranked Probability Score	$\frac{1}{n} \sum_{i=1}^n \sum_{j=1}^k (F_{1ij} - F_{2ij})^2$	The squared differences between cumulative predicted frequencies and observed frequencies, normalized by the number of observations [18].

Despite the many available options, no existing statistical tool measures both the direction and magnitude by which one distribution is shifted relative to another. First, existing measures of distance, divergence, intersection, and probabilistic scoring do not take directional values (Table 1) [3, 9, 18]. Second, while goodness-of-fit tests such as Mann-Whitney U, Wilcoxon signed-rank, and Kolmogorov-Smirnov can reveal significant one-tailed differences, the statistics of these and similar tests are not direct measures of distance, divergence, or intersection [3, 9]. Finally, none of these statistical tools are based on explicit measurement of shift (Table 1) [3, 9, 18].

The term shift is often used to describe directional changes in distributions or statistical moments [3, 5-7, 15]. However, some have attempted to define shift in more precise terms [4, 21]. For example, shift functions pertain to how and to what degree one distribution must be rearranged to match another [4, 21]. While shift functions are useful for visualization, they do not quantify shift with a single value in the way that, say, measures of distance quantify that property. Instead, shift functions rely on visual inspection, which sacrifices objectivity and precise measurement of the focal property [4, 21]. Shift functions may also be impractical when comparing many pairs of distributions.

In the present work, we define distributional shift (DS) as the concentration of frequencies towards the lowest discrete class, which we measure via the sum of cumulative frequencies. We then derive a relative measure (i.e., RDS) to reveal the direction and difference in shift between distributions, and then compare RDS to well established comparative measures (Table 1). Using simulations, we show how RDS can provide insights into healthcare billing practices. We then use a compilation of ~40,100 ecological samples to demonstrate DS as an advantageous measure of species rarity. Finally, using data on family incomes, poverty, and food

commodities, we demonstrate DS as a generalizable measure of poverty and scarcity, and as a natural complement to measures of inequality.

## 2. Approach

### 2.1 *Distributional shift (DS)*

A discrete frequency distribution,  $f$ , having  $n > 1$  observations distributed across  $k > 1$  discrete classes, hereafter bins, will have a cumulative form  $F$  such that  $n \leq \Sigma F \leq nk$  or, when normalized,  $1 \leq \Sigma F/n \leq k$ . When  $\Sigma F/n = 1$ , then  $f$  and  $F$  must be maximally shifted to the right, i.e., having values of 0 for all bins except the right-most. For example, letting  $k = 3$ :

$$\begin{aligned} \text{if } f &= [0, 0, n], \\ \text{then } F &= [0, 0, n], \\ \text{and } \Sigma F/n &= n/n = 1 \end{aligned}$$

Conversely, when  $\Sigma F/n = k$ , then  $F$  must have values of  $n$  for all bins and  $f$  must be maximally shifted to the left, i.e., having values of 0 for all bins except the left-most:

$$\begin{aligned} \text{If } f &= [n, 0, 0], \\ \text{then } F &= [n, n, n], \\ \text{and } \Sigma F/n &= (3 \cdot n) / n = 3 = k \end{aligned}$$

Subtracting 1 from  $\Sigma F/n$ , the resulting value represents the shift of  $f$  away from the right-most bin or, alternatively, towards the left-most bin:

$$\begin{aligned} \text{If } f &= [0, 0, n], \text{ then } \Sigma F/n = 1 - 1 = 0 \\ \text{If } f &= [n, 0, 0], \text{ then } \Sigma F/n = k - 1 = 2 \end{aligned}$$

Values of  $\Sigma F/n - 1$  can then be divided by  $k - 1$  to produce normalized values of distributional shift (DS) that range between 0 and 1, inclusive:

$$DS = (\Sigma F/n - 1) / (k - 1) \quad (1)$$

For example, given  $n = 3$  observations distributed among  $k = 3$  bins, let  $f_1 = [1, 1, 1]$  and  $f_2 = [2, 1, 0]$ . The cumulative forms of  $f_1$  and  $f_2$  are  $F_1 = [1, 2, 3]$  and  $F_2 = [2, 3, 3]$ , respectively.

Calculating DS for  $F_1$  and  $F_2$ :

$$\begin{aligned} DS(F_1) &= (\Sigma F_1/n - 1) / (k - 1) \\ &= (6/3 - 1) / (3 - 1) \\ &= 0.5 \\ DS(F_2) &= (\Sigma F_2/n - 1) / (k - 1) \\ &= (8/3 - 1) / (3 - 1) \\ &= 0.8\bar{3} \end{aligned}$$

Hence,  $f_2$  is shifted further left than  $f_1$ . More specifically,  $f_1$  is shifted to 50% of the possible maximum while  $f_2$  is shifted to ca. 83.3% of the possible maximum.

## 2.2 Correcting DS to obtain unique values

As formulated in equation 1, values of DS will not necessarily differ among non-identical distributions satisfying the same values of  $n$  and  $k$ . For example, consider the feasible set of all possible discrete cumulative frequency distributions for  $n = 3$  and  $k = 3$ , i.e.,  $A_{n=3,k=3}$ . Listed in lexicographical order, the 10 members of this feasible set and their values of DS are:

$$\begin{aligned} F_1 &= [0, 0, 3], & DS &= 0.0 \\ F_2 &= [0, 1, 3], & DS &= 0.1\bar{6} \\ F_3 &= [0, 2, 3], & DS &= 0.\bar{3} \\ F_4 &= [0, 3, 3], & DS &= 0.5 \\ F_5 &= [1, 1, 3], & DS &= 0.\bar{3} \\ F_6 &= [1, 2, 3], & DS &= 0.5 \end{aligned}$$

$$\begin{aligned}
F_7 &= [1, 3, 3], & \text{DS} &= 0.\overline{66} \\
F_8 &= [2, 2, 3], & \text{DS} &= 0.\overline{66} \\
F_9 &= [2, 3, 3], & \text{DS} &= 0.8\overline{33} \\
F_{10} &= [3, 3, 3], & \text{DS} &= 1.0
\end{aligned}$$

While all 10 members of  $A_{n=3,k=3}$  are unique, there are only 7 unique values of DS.

Consequently, two non-identical distributions could be interpreted as equally shifted towards the left-most bin. This property does not necessarily invalidate the measure, e.g., consider that two non-identical distributions can have the same mean, variance, etc. However, the issue can be resolved to ensure unique values of DS for non-identical distributions having the same  $n$  and  $k$ . Specifically, unique values of normalized sums can be achieved by exponentiating the cumulative frequencies to a power greater than 1, that is,  $\Sigma F^z$ , where  $z > 1$ . Normalized values can then be obtained using  $\Sigma F^z/n^z$ . For example, letting  $z = 2$  and considering the feasible set of discrete cumulative distributions for  $n = 3$  and  $k = 3$ :

$$\begin{aligned}
F_1 &= [0, 0, 3], & \Sigma F_1/n &= 1.00, & \Sigma(F_1^2)/n^2 &= 1.00 \\
F_2 &= [0, 1, 3], & \Sigma F_2/n &= 1.\overline{33}, & \Sigma(F_2^2)/n^2 &= 1.11 \\
F_3 &= [0, 2, 3], & \Sigma F_3/n &= 1.\overline{66}, & \Sigma(F_3^2)/n^2 &= 1.44 \\
F_4 &= [0, 3, 3], & \Sigma F_4/n &= 2.00, & \Sigma(F_4^2)/n^2 &= 2.00 \\
F_5 &= [1, 1, 3], & \Sigma F_5/n &= 1.\overline{66}, & \Sigma(F_5^2)/n^2 &= 1.22 \\
F_6 &= [1, 2, 3], & \Sigma F_6/n &= 2.00, & \Sigma(F_6^2)/n^2 &= 1.55 \\
F_7 &= [1, 3, 3], & \Sigma F_7/n &= 2.\overline{33}, & \Sigma(F_7^2)/n^2 &= 2.11 \\
F_8 &= [2, 2, 3], & \Sigma F_8/n &= 2.\overline{33}, & \Sigma(F_8^2)/n^2 &= 1.88 \\
F_9 &= [2, 3, 3], & \Sigma F_9/n &= 2.\overline{66}, & \Sigma(F_9^2)/n^2 &= 2.44 \\
F_{10} &= [3, 3, 3], & \Sigma F_{10}/n &= 3.00, & \Sigma(F_{10}^2)/n^2 &= 3.00
\end{aligned}$$

Here, each normalized sum of exponentiated cumulative frequencies, i.e.,  $\Sigma F^z/n^z$ , is unique and the original lower and upper constraints on  $\Sigma F/n$  are retained. Reformulating DS with respect to normalized sums of exponentiated cumulative frequencies:

$$\text{DS} = (\Sigma F^z/n^z - 1) / (k - 1) \quad (2)$$

Importantly, arbitrarily chosen exponents do not guarantee the uniqueness of  $\Sigma F^z/n^z$  among distributions with identical  $n$  and  $k$ . For example, consider the subset of the feasible set for  $n = 5$  and  $k = 4$ , where  $\Sigma F/n = 2.2$ :

$$\begin{aligned} F_1 &= [0, 1, 5, 5], & \Sigma F_1/n &= 2.2, & \Sigma(F_1^2)/n^2 &= 2.04, & \Sigma(F_1^3)/n^3 &= 2.008 \\ F_2 &= [0, 2, 4, 5], & \Sigma F_2/n &= 2.2, & \Sigma(F_2^2)/n^2 &= 1.8, & \Sigma(F_2^3)/n^3 &= 1.576 \\ F_3 &= [0, 3, 3, 5], & \Sigma F_3/n &= 2.2, & \Sigma(F_3^2)/n^2 &= 1.72, & \Sigma(F_3^3)/n^3 &= 1.432 \\ F_4 &= [1, 1, 4, 5], & \Sigma F_4/n &= 2.2, & \Sigma(F_4^2)/n^2 &= 1.72, & \Sigma(F_4^3)/n^3 &= 1.528 \\ F_5 &= [1, 2, 3, 5], & \Sigma F_5/n &= 2.2, & \Sigma(F_5^2)/n^2 &= 1.56, & \Sigma(F_5^3)/n^3 &= 1.288 \\ F_6 &= [2, 2, 2, 5], & \Sigma F_6/n &= 2.2, & \Sigma(F_6^2)/n^2 &= 1.48, & \Sigma(F_6^3)/n^3 &= 1.192 \end{aligned}$$

While using  $z = 2$  produces  $\Sigma F^z/n^z = 1.72$  for both  $F_3$  and  $F_4$ , unique values are obtained when using  $z = 3$ . Calculating DS for  $F_3$  and  $F_4$  produces  $DS(F_3) = 0.144$  and  $DS(F_4) = 0.176$ , which indicates that  $F_4$  is shifted left of  $F_3$ . However, this result may not be intuitive since a greater fraction of  $n$  is shifted left of center in  $F_3$ . Consequently, while larger exponents may produce unique values of  $\Sigma F^z/n^z$ , they can also inflate minor differences between distributions and produce questionable results (Fig 1). This undesirable effect can be avoided by using a fractional exponent. Specifically, using  $z = (k + 1)/k$  makes  $z$  dependent on  $k$  while avoiding large exponents (Fig 2). The equation for DS then becomes:

$$DS = (\Sigma F^{(k+1)/k} / n^{(k+1)/k} - 1) / (k - 1) \quad (3)$$

Although using  $z = (k + 1)/k$  produces unique values of DS for all combinations of  $n \leq 200$  and  $k \leq 20$  where  $|A_{n,k}| < 2 \cdot 10^7$ , we cannot mathematically prove that such will be the case for all combinations of arbitrarily large  $n$  and  $k$ . If it is not the case and if uniqueness is strictly necessary, then the exponent of DS will need to be revised.



**Figure 1.** Normalized sums of exponentiated cumulative frequencies ( $\Sigma F^z/n^z$ ) for distributions having 10 observations distributed among 5 bins, i.e.,  $A_{n=10,k=5}$ . This feasible set contains 1,001 distributions. While an exponent of  $z = 7$  produced unique values of  $\Sigma F^z/n^z$  for each distribution, distributions with equal values of  $\Sigma F/n$  had disparate values of  $\Sigma F^z/n^z$ .

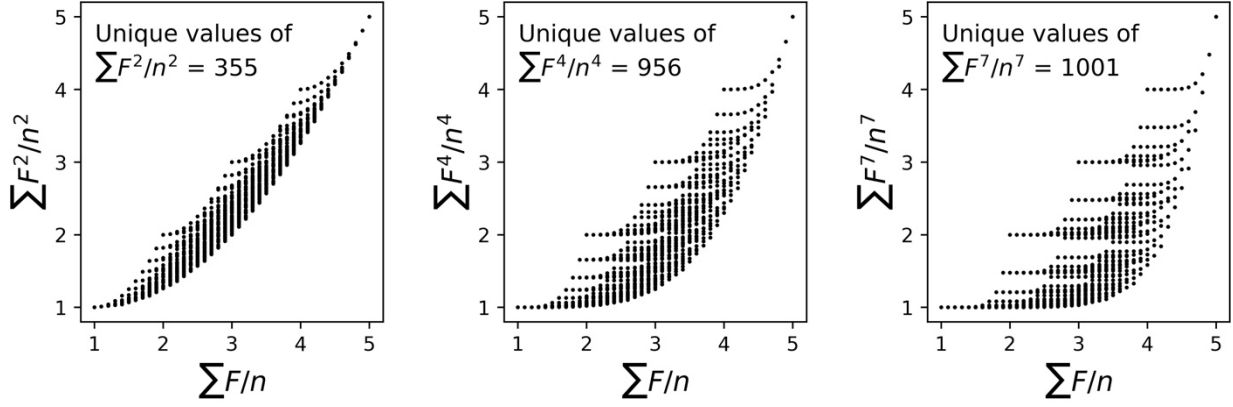
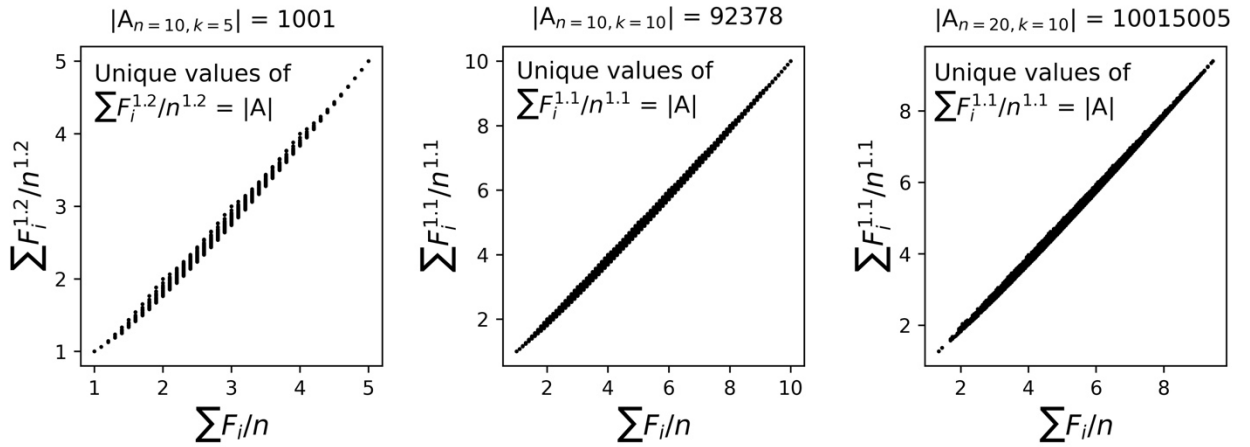


**Figure 2.** Normalized sums of exponentiated cumulative frequencies ( $\Sigma F^z/n^z$ ), where  $z = (k+1)/k$  and  $k$  is the number of bins and  $n$  is the number of observations. In each case, the number of unique values of  $\Sigma F^z/n^z$  equals the cardinality of the feasible set,  $|A|$ .



### 2.3. Relative distributional shift (RDS)

Given two discrete cumulative frequency distributions,  $F_1$  and  $F_2$ , having the same  $n$  and  $k$ , the distributional shift of  $F_1$  relative to  $F_2$  can be measured as a simple difference or relative distributional shift (RDS):

$$\text{RDS} = \text{DS}(F_2) - \text{DS}(F_1) \quad (4)$$

As the minimum possible value for DS is 0 and the maximum is 1, RDS is constrained to a minimum and maximum signed difference, i.e.,

$$-1 \leq \text{RDS} \leq 1.$$

The sign and magnitude of RDS then represents the degree to which  $F_1$  is shifted right or left of  $F_2$ . For example, given  $n = 10$ ,  $k = 3$ , and letting  $f_1 = [10, 0, 0]$  and  $f_2 = [0, 0, 10]$ :

$$F_1 = [10, 10, 10]:$$

$$\begin{aligned} \text{DS}(F_1) &= (\Sigma F_1^{(k+1)/k} / n^{(k+1)/k} - 1) / (k - 1) \\ &= [(3 \cdot 10^{(3+1)/3}) / 10^{(3+1)/3} - 1] / (3 - 1) \\ &= (3 - 1) / (3 - 1) = 1 \end{aligned}$$

$$F_2 = [0, 0, 10]:$$

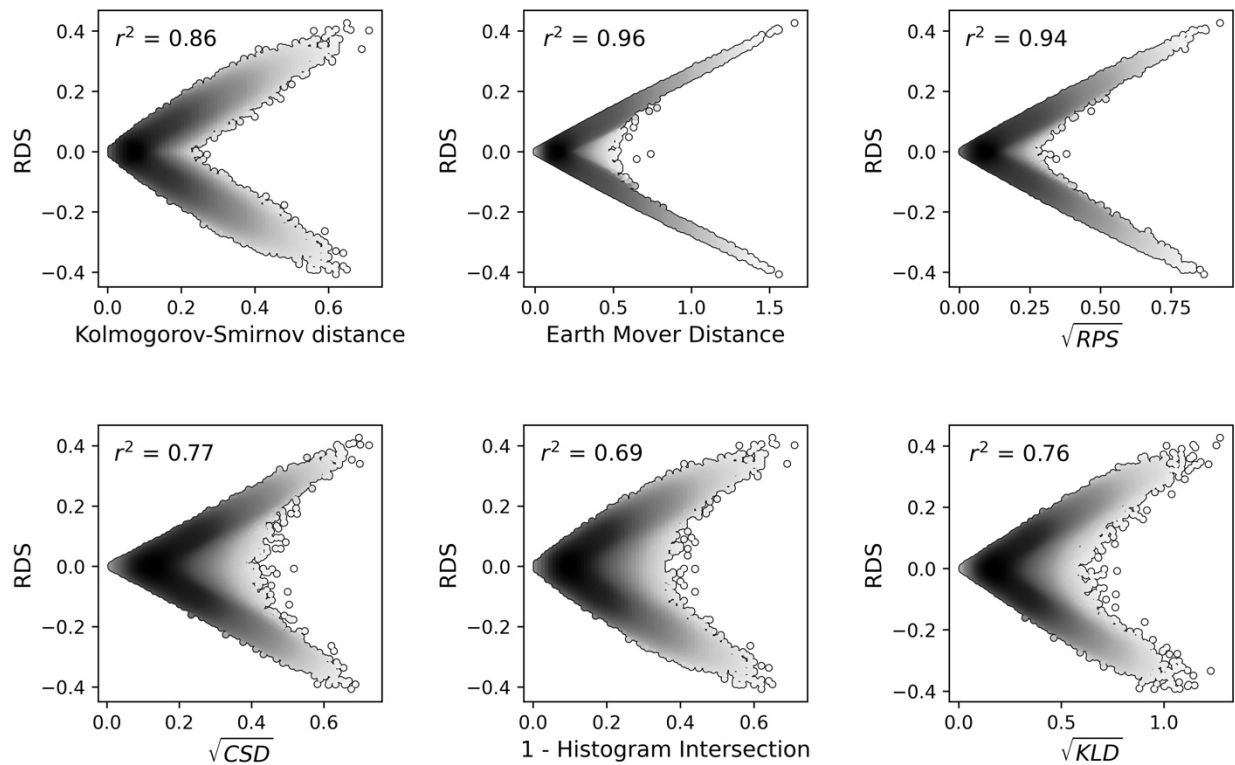
$$\begin{aligned} \text{DS}(F_2) &= (\Sigma F_2^{(k+1)/k} / n^{(k+1)/k} - 1) / (k - 1) \\ &= (10^{(3+1)/3} / 10^{(3+1)/3} - 1) / (3 - 1) \\ &= (1 - 1) / (3 - 1) = 0 \end{aligned}$$

Therefore,  $\text{RDS} = \text{DS}(F_2) - \text{DS}(F_1) = -1$ . The sign of RDS indicates that  $F_1$  is shifted left of  $F_2$ , while the absolute value of RDS takes the maximum possible absolute difference of 1. Taken together,  $F_1$  cannot be shifted more to the left of  $F_2$ .

## 2.4 Relationships of RDS to measures of distance, divergence, and intersection

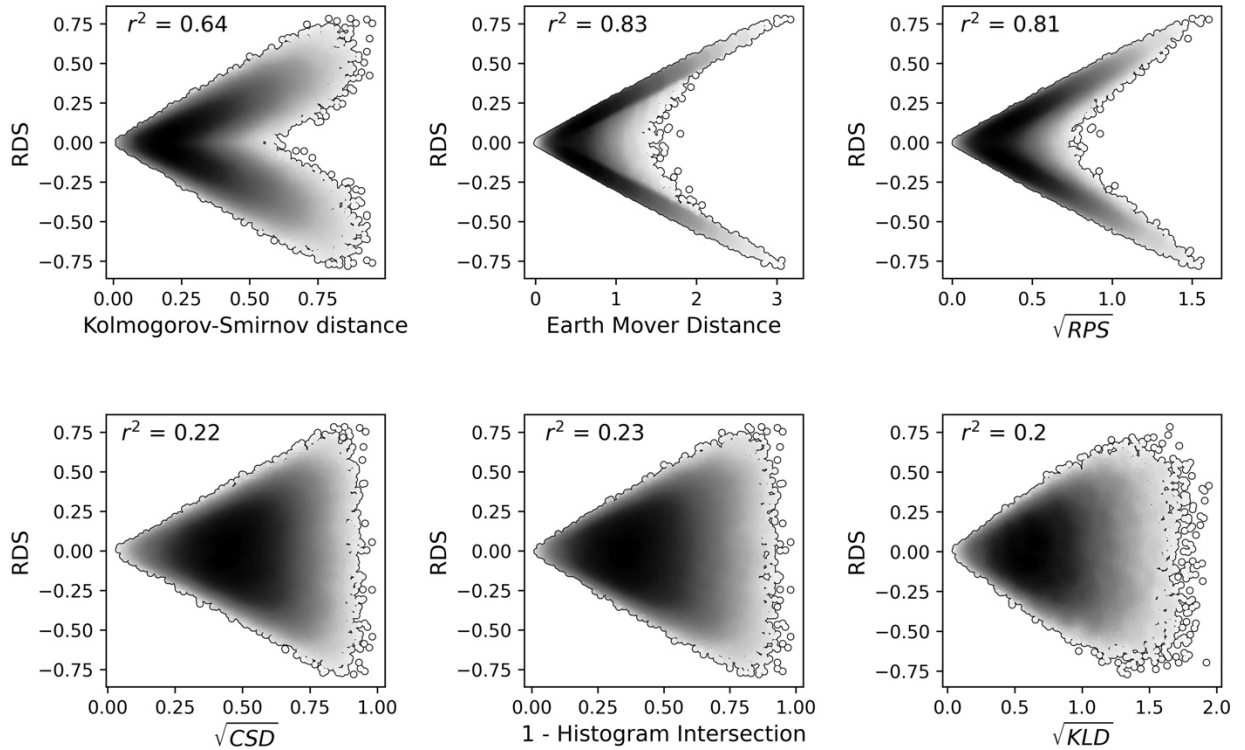
We examined relationships between RDS and Chi-square distance, Kullback-Leibler divergence, Kolmogorov-Smirnov distance, Earth Mover's distance, Ranked Probability Score, and histogram *non*-intersection (Table 1). Importantly, Kolmogorov-Smirnov distance, Earth Mover distance, and Ranked Probability Score (RPS) are, like RDS, based on the use of cumulative distributions. After calculating the above measures for  $10^5$  pairs of Poisson distributed random samples ( $\lambda = 5, n = 100, k = 5$ ), we found that RDS shared close relationships with other measures ( $0.7 \leq r^2 \leq 0.96, p < 0.001$ ) (Fig 3).

**Figure 3.** Relationships of Relative Distributional Shift (RDS) to Kolmogorov-Smirnov distance, Earth Mover distance, Ranked Probability Score (RPS), Chi-square distance (CSD), histogram non-intersection, and Kullback-Leibler divergence (KLD). Coefficients of determination ( $r^2$ ) were calculated using  $|RDS|$  and simple linear regression.



In contrast to the similar functional forms shared by Poisson distributed random samples, feasible sets contain all possible forms, many of which have disparate shapes [12]. Noting this, we calculated each of the above measures with respect to  $10^5$  randomly drawn pairs of distributions from the feasible set of 4,598,126 possible forms satisfying  $n = 100$  and  $k = 5$ . This time, RDS was only weakly related to Chi-square distance, histogram non-intersection, and Kullback-Leibler divergence ( $0.2 \leq r^2 \leq 0.23$ ) (Fig 4).

**Figure 4.** Relationships of Relative Distributional Shift (RDS) to Kolmogorov-Smirnov distance, Earth Mover distance, Ranked Probability Score (RPS), Chi-square distance (CSD), histogram non-intersection, and Kullback-Leibler divergence (KLD). Coefficients of determination ( $r^2$ ) were calculated using  $|RDS|$  and simple linear regression.



RDS often remained near zero when values of Chi-square distance, histogram non-intersection, and Kullback-Leibler divergence were high (Fig 4). This result emerged for two reasons. First, unlike these latter measures, RDS is based on the analysis of cumulative distributions, which are often preferred as they are less sensitive to outliers and are more stable than non-cumulative forms [16, 22]. Coincidentally, Kolmogorov-Smirnov distance, Earth Mover's distance, and Ranked Probability Score are also based on cumulative distributions, which likely explains their strong relationships to RDS (Fig 3, 4). Second, as demonstrated below, differences in shape do not imply differences in shift.

Letting  $n = 46$  observation be distributed among  $k = 5$  bins, consider the case when  $f_1 = [21, 2, 0, 2, 21]$  and  $f_2 = [1, 1, 42, 1, 1]$ . For  $f_1$ ,  $\sim 45.7\%$  of  $n$  is shifted entirely left while nearly  $45.7\%$  remains in the right-most bin, essentially splitting  $91.3\%$  of  $n$  between the left-most and right-most bins. For  $f_2$ , nearly  $91.3\%$  of  $n$  is shifted  $50\%$  left, basically splitting the difference present in  $f_1$ . Because of this, DS for  $f_1$  and  $f_2$  are similar,  $DS(f_1) = 0.435$ ,  $DS(f_2) = 0.489$ , resulting in a low value for RDS (0.053) despite the disparate shapes of  $f_1$  and  $f_2$ . Calculating the histogram non-intersection for  $f_1$  and  $f_2$  produces  $91.3\%$  non-overlap. Hence,  $f_1$  and  $f_2$  are distributions with disparate shapes but similar shift.

### 3. Application

#### 3.1 Healthcare: Using RDS to examine billing practices

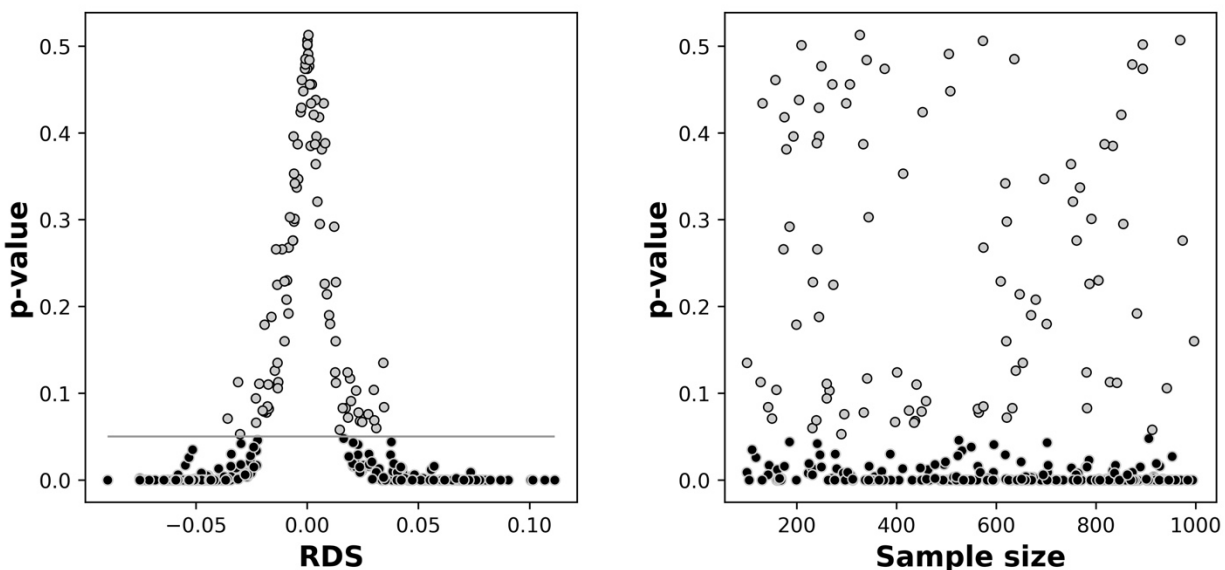
Evaluation and Management (E/M) coding profiles are ordinal distributions of office visits that break down a healthcare provider's patient encounters across a series of billing codes, whereby higher codes correspond to greater clinical complexity [20]. These profiles have expected forms based on clinical specialties; comparisons to which serve as the basis for audits by private and

governmental insurance carriers [20]. While deviations from expected profiles may result from the idiosyncrasies of a provider's patient panel, a profile that is shifted left of its expectation can indicate that a provider has been under-billing for services while a profile that is shifted right may indicate that a provider is over-billing.

Here, we demonstrate how RDS can be used to rank providers, from potential under-billers to potential over-billers. We simulated a hospital having 50 clinical specialties equally distributed among 300 providers. Each specialty's expected coding profile was simulated by parameterizing a Poisson distribution with a random value ( $1.5 \leq \lambda \leq 3$ ). Normalizing the resulting distributions produced coding profiles with internal modes among five classes, similar to expected forms [20]. To simulate coding profiles for each provider, we drew Poisson-distributed random samples of  $10^2$  to  $10^3$  observations with  $\lambda$  chosen at random within 80% to 120% of the expectation.

We derived one-sided  $p$ -values for each provider's coding profile by resampling their expected profile  $10^4$  times according to their simulated number of office visits and calculating the resulting RDS values. We then plotted each provider's RDS value against their empirical  $p$ -value. We found that values of RDS quickly became significant as they departed from 0 (Fig 5). Using a significance value of 0.05, all simulated profiles were significantly shifted whenever the absolute value of RDS was more than 5% of the maximum (Fig 5). This approach of empirically deriving one-sided  $p$ -values was also independent of sample size, i.e., numbers of simulated office visits (Fig 5). Had these been real data, the hospital could have easily identified providers with E/M coding profiles that were significantly shifted towards lower or higher billing codes relative to expected clinical benchmarks.

**Figure 5.** Left: Statistical significance versus relative distributional shift (RDS). Black dots represent physician's with significant  $p$ -values. Gray dots represent physicians with non-significant  $p$ -values. The horizontal gray line represents the  $\alpha$  value. Right:  $p$ -values versus sample size, i.e., simulated numbers of office visits.



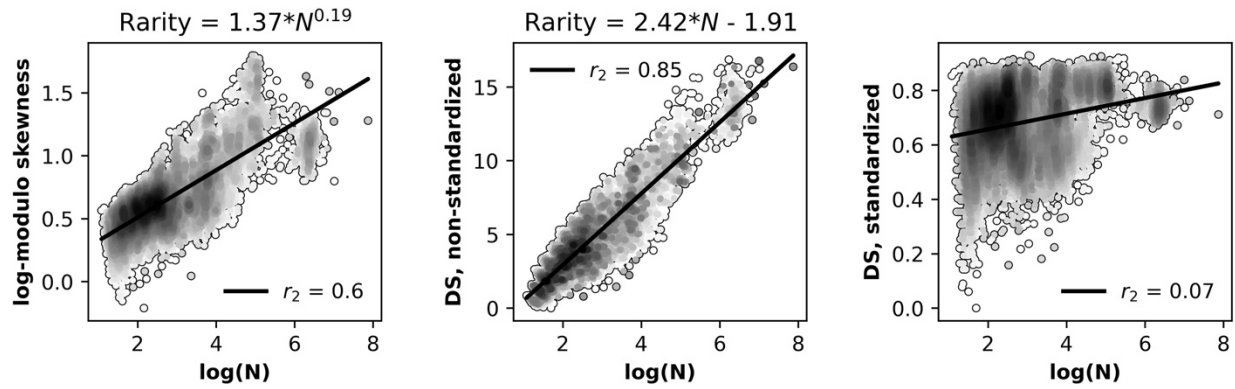
### 3.2 Ecology: *DS as a measure of species rarity*

A species abundance distribution (SAD) is a histogram of abundances sampled from an ecological community, e.g., trees of a forest, mammals of a desert, bacteria of a pond [14]. SADs underpin thousands of ecological studies and are the basis for many biodiversity measures [9-12, 14-16, 19, 22]. In particular, species rarity ( $R$ ) is often based on an SAD's skewness [16, 10, 11]. However, unbounded measures of skewness defy intuitive interpretation. Moreover, skewness is actually a measure of asymmetry, and may conflate the shape of an SAD with its concentration of species towards the lowest possible abundance class.

Here, we demonstrate the use of DS as a measure of species rarity using data from a study of ~40,100 communities of plants, animals, fungi, and bacteria [10]. That study measured

$R$  via a log-modulo transformation of skewness and supported the statistical scaling of  $R$  with total sample abundance ( $N$ ):  $R \propto N^z$  [10]. Reanalyzing that study's data, the non-standardized form of DS (i.e.,  $\Sigma F^{(k+1)/k} / n^{(k+1)/k} - 1$ ) explained  $\sim 85\%$  of variation in  $\log(N)$  compared to  $\sim 60\%$  of variation explained via the skewness-based measure (Fig 6). See Appendix 1 for methodological details.

**Figure 6.** Relationships of species rarity to total sample abundance ( $N$ ). Left: A previously documented rarity-abundance scaling relationship [10, 11]. Center: Rarity measured as a non-standardized version of distributional shift (DS). Right: Rarity measured as the standardized version of DS, the values of which are constrained to between 0 and 1.



The standardized form of DS, i.e.,  $(\Sigma F^{(k+1)/k} / n^{(k+1)/k} - 1) / (k - 1)$ , was however poorly related to  $N$  (Fig 6). This result emerges because the abundance of the most abundant species ( $N_{max}$ ) strongly scales with  $N$  and because an arbitrarily large increase in  $N$  will increase the number of bins in the SAD [11]. By dividing the non-standardized measure of DS (i.e.,  $\Sigma F^{(k+1)/k} / n^{(k+1)/k} - 1$ ) by the number of bins, the standardized measure lessens the indirect influence of  $N$  on rarity. While the standardized measure provides a weaker relationship to  $N$ , it is the preferred measure when the effect of  $N$  is to be controlled for.



### 3.3 Economics: *DS as a measure of poverty and scarcity*

Numerous measures can be used to examine distributions of wealth on the basis of inequality and poverty (Table 2) [8, 28]. However, while measures of inequality such as the Gini index are solely based on statistical dispersion, measures of poverty invariably use an arbitrated poverty line (Table 2) [8, 28]. Consequently, and unlike inequality measures, poverty cannot be easily calculated for distributions of wealth based on assets, commodities, natural resources, human capital, or family incomes for different nations.

**Table 2.** Poverty measures. Each relies on a poverty line. The poverty rate, poverty gap index, and poverty severity index belong to the family of Foster–Greer–Thorbecke indices [8].

Measure	Equation	Description
Poverty rate, i.e., head count ratio	$P_0 = \frac{N_p}{N}$	The number of impoverished people, families, etc. ( $N_p$ ) divided by the number of people, families, etc. ( $N$ ) [8].
Poverty Gap Index	$P_1 = \frac{1}{N} \sum_{i=1}^N \frac{G_i}{z}$	Normalized sum of ratios between individual poverty gaps ( $G_i$ ) and the poverty line ( $z$ ), where $G_i = z - y_i$ and $y_i$ is the income of the $i^{\text{th}}$ individual, family, etc. [8].
Poverty Severity Index	$P_2 = \frac{1}{N} \sum_{i=1}^N \left( \frac{G_i}{z} \right)^2$	Similar to the $P_1$ but based on a normalized sum of squares [8].
Sen Index	$P_S = P_0 \left( 1 - (1 - G^P) \frac{\mu^P}{z} \right)$	A combination of poverty rate ( $P_0$ ) and Gini's inequality index ( $G$ ), where $G^P$ is inequality among the poor and $\mu^P$ is the mean income among the poor [8].
Sen-Shorrocks-Thon Index	$P_{SST} = P_0 P_1^P (1 + \hat{G}^P)$	The product of poverty rate, the poverty gap index (only including the poor), and 1 plus the Gini coefficient of the poverty gap ratios for the entire population [8].
Watts Index	$W = \frac{1}{N} \sum_{i=1}^P \ln \left( \frac{z}{y_i} \right)$	Normalized sum of logarithmically transformed ratios of the poverty line ( $z$ ) to individual income ( $y_i$ ) for all individuals qualifying as poor ( $P$ ) [8].

US poverty lines were established in the 1960's and are based on estimated costs of adequate food intake for a family of a given size [8]. This estimate is updated annually and is multiplied by 3 to derive the poverty line [8]. Though highly oversimplified, US poverty lines are used to determine whether households qualify for federal assistance [8, 27]. Similarly oversimplified is the means by which US poverty is commonly reported, i.e., the poverty rate (Table 2). Although intuitive, the poverty rate does not reveal how poor the poor are when compared to the rest of the population, i.e., relative poverty.

We examined the potential of DS as a distributional measure of poverty using data on family incomes and US poverty rates from the United States Census Bureau [25, 26]. These data included 13 census years (2010-2022) and 16 bins of 2020 inflation-corrected family incomes (see Appendix 2). From these data, we used five categories of single race/ethnicity households: Hispanic or Latinx, White not Hispanic or Latinx, Asian, Black or African American, Native American or Alaskan Native.

Despite being based on highly aggregated data and no poverty lines, longitudinal patterns of DS largely reflected those of US poverty rates (Fig 7). Since 2010, Native American, Alaska Native, and Black or African American families have experienced far greater poverty than Asian and White non-Hispanic/Latinx families (Fig 7). While White non-Hispanic/Latinx families had the lowest poverty rates, Asian families had the lowest shift towards poverty, a result of higher affluency among Asian families (Fig 7). While official US poverty rates have generally decreased since 2010, DS revealed that the poorest families have gotten poorer, especially since the onset of COVID-19 (Fig 8). In contrast, low-to-middle income families have shifted away from poverty (reversing some racial differences) while middle-to-high income families have shifted to greater affluency (largely maintaining racial differences) (Fig 8).

**Figure 7.** Left: Official US poverty rates. Center: Poverty measured as distributional shift (DS). Right: Affluency rate, measured as the percent of families with annual incomes  $\geq$  \$200K.

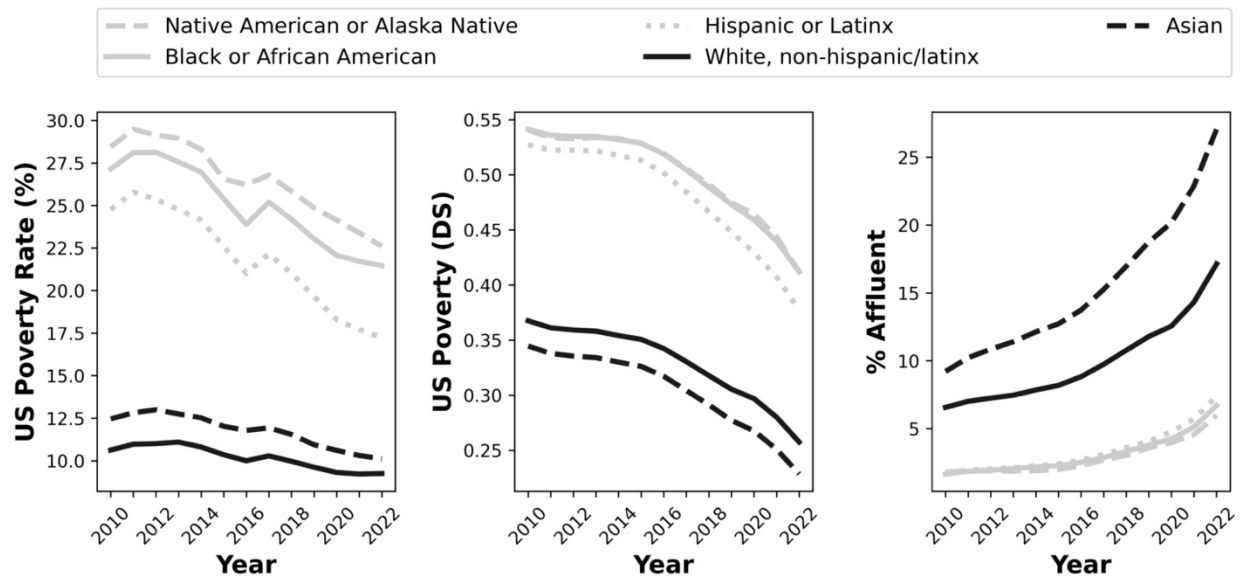
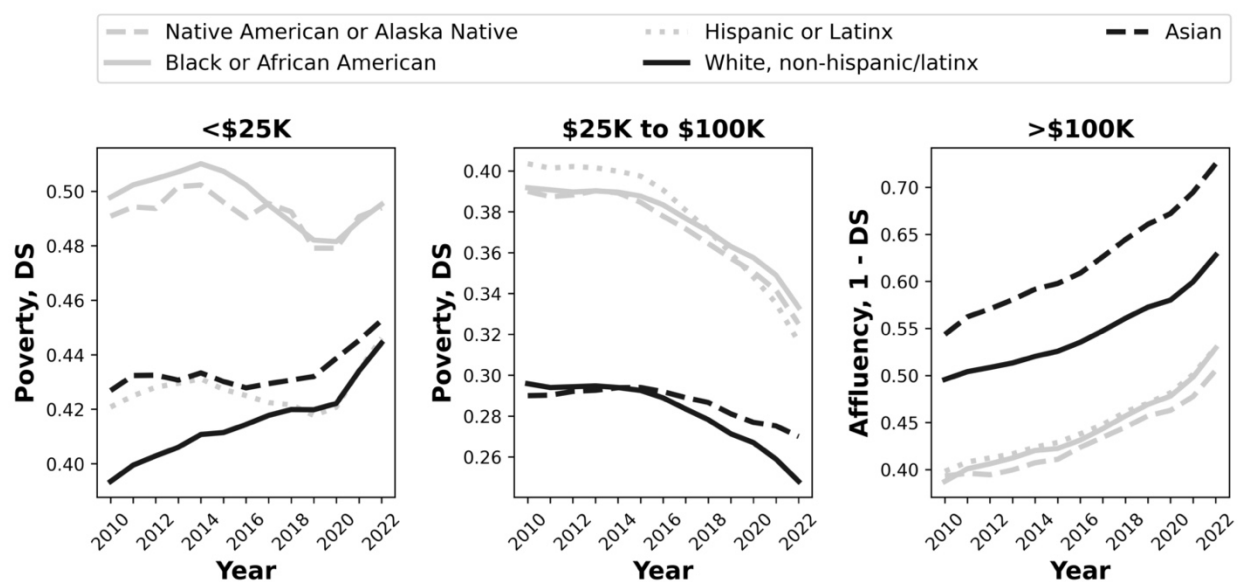
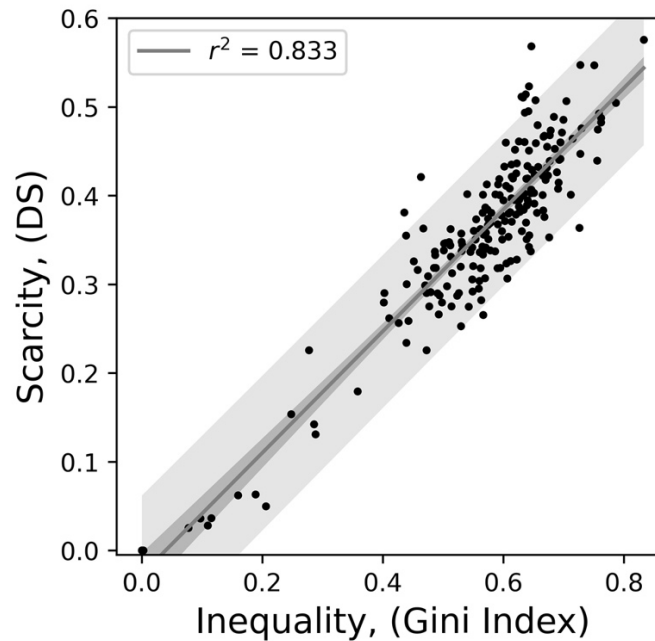


**Figure 8.** Poverty measured as distributional shift (DS). Left: Families with annual incomes less than \$25K. Note the abrupt increase in poverty between 2020 and 2022. Center: Families with annual incomes between \$25K and \$100K. Right: Families with incomes greater than >\$100K.



Next, we examined DS as a measure of scarcity using data on the production of 209 food commodities (e.g., wheat, rice, chicken meat) among 200 nations in 2022. We obtained these publicly available data from the United Nations Food and Agriculture Organization website [24]. We calculated DS and the Gini coefficient of inequality with respect to each food commodity (See Appendix 3). As could have been expected, greater inequality in food production was positively associated with greater scarcity and hence, a greater fraction of nations that produced relatively little ( $r^2 = 0.833$ ) (Fig 9). However, scarcity sometimes took a considerable range of values for a given value of inequality. For example, at an inequality of  $\sim 0.62$ , scarcity ranged from nearly 0.3 to nearly 0.56 (Fig 9). As two distributions with similar inequality can greatly differ in scarcity, both are important to quantify.

**Figure 9.** Scarcity of food production, measured as DS versus inequality in food production. Each dots represents one of 209 food commodities.



#### 4. Discussion

The notion of shift is commonly invoked in the analysis of frequency distributions but is rarely defined in precise terms or as a statistical property *per se* [3-7, 15, 18, 21]. In the current study, we defined distributional shift (DS) as the concentration of a distribution towards the left-most discrete class, which is quantified using the normalized sum of exponentiated cumulative frequencies. We then defined a measure, RDS, to reveal the magnitude and direction by which one distribution is shifted relative to another. Realizing the link between DS and concepts of rarity, poverty, and scarcity, we demonstrated advantages of using DS as an alternative or complementary measure of these properties. To the best of our knowledge, no other measure of rarity, poverty, or scarcity can be interpreted as a general property of distributional shift, whether for distributions of wealth and abundance, or otherwise.

Aside from its explicit focus on shift, the measurement of RDS differs importantly from measures of distance, divergence, intersection, and probabilistic scoring. Specifically, these measures have a shared property in their calculations that prevents them from taking signed (i.e., directional) values; specifically, pairwise differences in the frequencies of corresponding bins or discrete classes. In contrast, RDS compares distributions in their entirety, producing a simple signed difference to which statistical significance can be attributed. Despite this novel characteristic, values of RDS were often highly related to those of other measures. Consequently, investigators seeking thorough comparisons via the use of multiple measures, each capturing a subtly different property, can capitalize on RDS for its unique focus on shift and its unique ability to take signed values.

The use of DS as the basis for both a general comparative measure of discrete frequency distributions and as a descriptive measure of rarity, poverty, and scarcity begs an interesting

question. Specifically, if DS is an appropriate measure of rarity, poverty, and scarcity (which it seems to be) and if values of RDS are highly related to those of popular measures such as Kolmogorov-Smirnov distance, Earth Mover distance, and Ranked Probability Score (which they are), then to what degree do these long-established measures compare distributions on the basis of rarity, poverty, and/or scarcity? It is likewise interesting that, unlike RDS, these popular measures cannot be decomposed into elements, such as DS, that reflect the rarity, poverty, or scarcity of each distribution.

### **Acknowledgments**

We thank Dr.'s Ethan P. White and Xiao Xiao for providing valuable feedback and fruitful discussions, in particular, on the comparison of RDS to other measures. We also thank the individuals who collected and provided the many ecological datasets that comprise the large data compilation used herein [see 10].

### **Availability of data and source code**

All data and source code needed to reproduce the findings and figures herein are available in a public institutional repository: [https://github.com/Rush-Quality-Analytics/distributional\\_shift](https://github.com/Rush-Quality-Analytics/distributional_shift).

### **Disclosure statement**

No potential conflict of interest was reported by the authors.

### **References**

1. V. Asha, N.U. Bhajantri, and P. Nagabhushan. GLCM-based chi-square histogram distance for automatic detection of defects on patterned textures. *Int. J. Comput. Vision. Robot.* 2 (2011), pp. 302-313.

2. S.I. Bityukov, A.V. Maksimushkina, and V.V. Smirnova. Comparison of histograms in physical research. *Nucl. Energ. Technol.* 2 (2016), pp. 108-113.
3. M.M. Deza and E. Deza. *Encyclopedia of distances*. Springer Berlin Heidelberg, 2009.
4. K. Doksum. Empirical probability plots and statistical inference for nonlinear models in the two-sample case. *Ann. Statist.* 2 (1974), pp. 267-277.
5. X. Du, D.A. Hennessy, and C.L. Yu. Testing Day's conjecture that more nitrogen decreases crop yield skewness. *Am. J. Agric. Econ.* 94 (2012), pp. 225-237.
6. S. Duffy, J. Huttenlocher, L.V. Hedges, and L.E. Crawford. Category effects on stimulus estimation: Shifting and skewed frequency distributions. *Psychon. Bull. Rev.* 17 (2010), pp. 224-230.
7. S. Fattorini, T. Di Lorenzo, and D.M.P. Galassi. Earthquake impacts on microcrustacean communities inhabiting groundwater-fed springs alter species-abundance distribution patterns. *Sci. Rep.* 8 (2018), pp. 1501.
8. J. Haughton and S.R. Khandker. *Handbook on poverty + inequality*. World Bank Publications; 2009 Mar 27. pp. 446.
9. P. Legendre and L. Legendre. *Numerical ecology*. Elsevier, 2012.
10. J.T. Lennon and K.J. Locey. More support for Earth's massive microbiome. *Biol. Direct.* 15 (2020), 1-6.
11. K.J. Locey and J.T. Lennon. Scaling laws predict global microbial diversity. *Proc. Natl. Acad. Sci. USA.* 24 (2016), pp. 5970-5975.
12. K.J. Locey and E.P. White. How species richness and total abundance constrain the distribution of abundance. *Ecol. Lett.* 16 (2013), pp. 1177-1185.

13. B.B. Luczak, B.T. James, and H.Z. Girgis. A survey and evaluations of histogram-based statistics in alignment-free sequence comparison. *Brief. Bioinform.* 20 (2019), pp. 1222-1237.
14. B.J. McGill, R.S. Etienne, J.S. Gray, D. Alonso, M.J. Anderson, H.K. Benecha, M. Dornelas, B.J. Enquist, J.L. Green, F. He, A.H. Hurlbert, A.E. Magurran, P.A. Marquet, B.A. Maurer, A. Ostling, C.U. Soykan, K.I. Ugland, and E.P. White. Species abundance distributions: moving beyond single prediction theories to integration within an ecological framework. *Ecol. Lett.* 10 (2007), pp. 995-1015.
15. D.J. McGlinn, X. Xiao, F. May, N.J. Gotelli, T. Engel, S.A. Blowes, T.M. Knight, O. Purschke, J.M. Chase, and B.J. McGill. Measurement of Biodiversity (MoB): A method to separate the scale-dependent effects of species abundance distribution, density, and aggregation on diversity change. *Methods. Ecol. Evol.* 10 (2019), pp. 258-269.
16. A.E. Magurran and B.J. McGill, eds. *Biological diversity: frontiers in measurement and assessment*. OUP Oxford, 2010.
17. D. Monrad, E.J. Harner, and W.F. Stout. *Statistics Concepts & Methods*. 4th ed. Dubuque, IA: Kendall Hunt; 2010.
18. A.H. Murphy. The ranked probability score and the probability score: A comparison. *Mon. Weather. Rev.* 98 (1970), pp. 917-924.
19. J.C. Nekola and J.H. Brown. The wealth of species: ecological communities, complex systems and the legacy of Frank Preston. *Ecol. Lett.* 10 (2007), pp. 188-96.
20. B. Nicoletti. How to analyze your E/M coding profile. *Fam. Pract. Manag.* 14 (2007), pp. 39-43.



21. G.A. Rousselet, C.R. Pernet, and R. Rand. Wilcox. Beyond differences in means: robust graphical methods to compare two groups in neuroscience. *Eur. J. Neurosci.* 46 (2017), pp. 1738-1748.
22. J.L. Simonis, E.P. White, and S.K.M. Ernest. Evaluating probabilistic ecological forecasts. *Ecology.* 102 (2021), e03431.
23. J.S. Simonoff and F. Udina. Measuring the stability of histogram appearance when the anchor position is changed. *Comput. Stat. Data. Anal.* 23 (1997), pp. 335-353.
24. United Nations, Food and Agriculture Organization. FAOSTAT. Crops and livestock products. <https://www.fao.org/faostat/en/#data/QCL>. Accessed, 24 Feb, 2024.
25. United States Census Bureau. American Community Survey 1-Year Estimates: Income in the Past 12 Months (Households, Families, Individuals). <https://data.census.gov>. Accessed, 18 Feb, 2024.
26. United States Census Bureau. American Community Survey 1-Year Estimates: Poverty Status in the Past 12 Months. U.S. Census Bureau. <https://data.census.gov>. Accessed, 22 Feb, 2024.
27. United States Department of Health and Human Services. Programs that Use the Poverty Guidelines as a Part of Eligibility Determination. <https://www.hhs.gov/answers/hhs-administrative/what-programs-use-the-poverty-guidelines/index.html>. Accessed, 27 Feb, 2024.
28. R.F Williams and D.P. Doessel. Measuring inequality: tools and an illustration. *Int. J. Equity Health.* 5 (2006), pp. 1-8.

## Appendices

### **Appendix 1. Analysis of species abundance distributions and the use of distributional shift (DS) as a measure of species rarity.**

We used a previously published global-scale data compilation of nearly 40,100 samples from geographically unique sites of ecological communities of plants, animals, fungi, archaea, and bacteria [10]. The data from that study are publicly available and likewise compiled from large-scale sampling projects, and were primarily used for the analysis of ecological scaling laws and the prediction of global biodiversity [10, 11]. In the data, each sample was represented by a vector of species abundances, which could then be analyzed as a frequency distribution, i.e., a species-abundance distribution (SAD). Using the data from references 10 and 11, we calculated our measure of distributional shift (DS) for each sample having 10 or more species. In general, SADs with less than 10 species are not considered sufficient for analysis [11]. We also calculated the studies' original measure of species rarity ( $R$ ), i.e., log-modulo skewness:

$$R = \log_{10}(|\gamma| + 1), \text{ if } 0 \leq \gamma$$

$$R = -\log_{10}(|\gamma| + 1), \text{ if } \gamma < 0$$

Importantly, we calculated DS based on SADs with  $\log_2$  abundance classes as opposed to arithmetic abundance classes. The use of logarithmic abundance classes is a common practice in ecological studies [16] and offered greater analytical efficiency, i.e., since an SAD with a maximum species abundance of, e.g.,  $10^4$ , would have that many discrete abundance classes, the vast majority of which would be empty. However, on the  $\log_2$  scale there would only be 14 discrete abundance classes.

## **Appendix 2. Analysis of US poverty rates, family incomes, and the use of distributional shift (DS) as a measure of poverty.**

We examined distributional shift (DS) as a measure of poverty using data from the US Census Bureau on family incomes and poverty rates, from 2010 to 2022 [25, 26]. Family income data included 16 bins of inflation-corrected annual family incomes (Table A1).

**Table A1.** 16 bins of inflation-corrected annual family incomes. These bins are not of equal width. Results are given for the year 2022, which included data from 81,432,908 families.

<b>Income bin</b>	<b>No. of families included in 2022</b>	<b>% of total in 2022</b>
\$0 to \$10,000	2,503,187	3.07392559
\$10,000 to \$14,999	1,498,443	1.84009516
\$15,000 to \$19,999	1,600,812	1.96580478
\$20,000 to \$24,999	2,028,300	2.49076208
\$25,000 to \$29,999	2,236,899	2.74692265
\$30,000 to \$34,999	2,386,079	2.93011640
\$35,000 to \$39,999	2,463,465	3.02514678
\$40,000 to \$44,999	2,525,965	3.10189709
\$45,000 to \$49,999	2,616,615	3.21321572
\$50,000 to \$59,999	5,242,942	6.43835782
\$60,000 to \$74,999	7,445,194	9.14273378
\$75,000 to \$99,999	11,250,047	13.81511145
\$100,000 to \$124,999	9,364,651	11.49983615
\$125,000 to \$149,999	7,122,680	8.74668506
\$150,000 to \$199,999	9,059,762	11.12543101
\$200,000 or greater	12,087,867	14.84395842

### **Appendix 3. Analysis of distributions for the production of food commodities among nations in 2022.**

We examined distributional shift (DS) as a measure of scarcity with respect to the production of food commodities (e.g., wheat, rice, chicken meat) among nations. Food production was reported in numbers of metric tons. We calculated DS and the Gini coefficient of inequality with respect to each food commodity. The Gini coefficient is the most commonly used measure of economic inequality and is equal to the area under the Lorenz curve, i.e., a plot of cumulative wealth (e.g., income) versus the cumulative portion of a sample (e.g., set of nations) [8, 28]:

$$Gini = 1 - \sum_{i=1}^N (x_i - x_{i-1}) (y_i + y_{i-1})$$

The Gini coefficient largely reflects a transformation of the sample variance, bounded between 0 (all values are equal) and 1 (one non-zero observation and an infinite number of 0-valued observations). As with our ecological analyses of species-abundance distributions, we calculated DS using logarithmically-scaled ( $\log_2$ ) bins. We calculated the Gini coefficient using a square root transformation on observed values, as it produced a strong linear relationship to DS, whereas raw values or log-scaled values produced weaker, curvilinear relationships.